

# ***In situ* observation of gas-source molecular beam epitaxy of silicon and germanium on Si(001)**

I. Goldfarb,<sup>a)</sup> J. H. G. Owen, D. R. Bowler, C. M. Goringe, P. T. Hayden, K. Miki, D. G. Pettifor, and G. A. D. Briggs

*Department of Materials, University of Oxford, Oxford OX1 3PH, England*

(Received 26 September 1997; accepted 23 February 1998)

We have observed the development of the surfaces during gas-source growth of silicon and germanium in an elevated temperature ultrahigh vacuum scanning tunneling microscopy (STM), with near-atomic resolution under a range of temperature and flux, which are the two dominant parameters, and applied atomistic modeling to the structures seen by STM to enable us to give confident interpretation of the results. A key role in the growth of silicon and germanium on Si(001) from disilane and germane, respectively, is played by the surface hydrogen. The growth of germanium follows a similar path to that of silicon for the first few monolayers, after which the strain becomes relieved by periodic trenches, and eventually by a combination of faceted pits and clusters, both of which nucleate heterogeneously at surface defects. Understanding these processes is crucial to controlling the self-assembled Ge/Si quantum structures. © 1998 American Vacuum Society. [S0734-2101(98)56903-5]

## **I. INTRODUCTION**

Due to its compatibility with silicon technology, the Si-Ge alloy system is highly attractive for the fabrication of semiconductor devices, e.g., in the field of high-speed heterojunction bipolar transistors. However, full exploitation of epitaxially grown SiGe alloys on Si in planar device technology is hindered by the mismatch strain in this system, which causes three-dimensional (3D) roughness and/or misfit dislocations.<sup>1-3</sup> On the other hand, the 3D features which arise during roughening are self-assembled, and thus can be useful in low-dimensional quantum-confined devices.<sup>4,5</sup> For any uses it is invaluable to be able to control the morphology of the interface at the atomic scale.

Si on Si(001) is a model system for layer-by-layer epitaxial growth, whereas Ge on Si(001) is a model system for the Stranski-Krastanow growth, where the initial two-dimensional (2D) wetting layer grows pseudomorphically until the strain due to the 4.2% of lattice mismatch is elastically relaxed via the formation of 3D islands,<sup>1,2</sup> or ripples.<sup>3</sup> In this work, we make a comparison between silicon and germanium growth. The mismatch between the epitaxial Ge layer and the Si substrate, and the 50 °C difference in hydrogen desorption temperature between Si(001) and Ge(001) (Ref. 6) affect the kinetics of nucleation, and the growth modes of Ge/Si(001). We, therefore, investigate these two systems to learn about strained-layer growth in general, and to achieve a better control over the growth of Si<sub>1-x</sub>Ge<sub>x</sub>/Si alloys, in particular.

The growth of silicon using gas-source molecular beam epitaxy (GSMBE) from silane (SiH<sub>4</sub>) (Ref. 7) and disilane (Si<sub>2</sub>H<sub>6</sub>) (Ref. 8) has previously been studied using room-temperature scanning tunneling microscopy (STM) after annealing; GSMBE was chosen since in Ge/Si(001) growth the hydrogen (which is inherent to the hydride decomposition on

silicon surfaces) is known to reduce the undesired effects of Ge segregation and Si-Ge intermixing.<sup>9</sup> In previous work, we have studied by real-time elevated-temperature scanning tunneling microscopy nucleation processes of small islands<sup>10</sup> and, at a larger scale, the effect of hydrogen on the growth modes of silicon (Ref. 11) and germanium.<sup>12-14</sup> Mo and Lagally<sup>15</sup> were the first to show that in the low-coverage limit the MBE growth of Ge is very similar to that of Si. However, the presence of hydrogen on the surface has a profound effect not only as a diffusion blocker,<sup>11,14,16</sup> but also as a possible surfactant, which can bind to island and step edges,<sup>11</sup> promoting various instabilities<sup>17</sup> and different scaling laws,<sup>18</sup> and thus GSMBE growth could, in principle, yield a different comparison. Our previous work has nevertheless demonstrated many similarities between the Ge and Si growth patterns at the low-coverage/low-temperature limits.<sup>14</sup> The present work expands on our previous work demonstrating that there are also differences between Ge and Si in the kinetics of nucleation of 2D islands.

## **II. EXPERIMENTAL AND THEORETICAL METHODS**

Detailed descriptions of our experimental and theoretical methods can be found elsewhere (e.g., see Refs. 10 and 14). Briefly, following *ex vacuo* chemical treatment the Si substrates were degassed in UHV, flashed at 1150 °C, and slowly cooled to the desired temperature. A JEOL JSTM-4500XT capable of operation up to 1200 °C was used to monitor the growth *in situ*, by separately exposing the sample mounted in the STM stage to disilane and germane in the room-temperature (RT)-450 °C K temperature and 10<sup>-7</sup>-10<sup>-5</sup> Pa pressure ranges. The STM imaging was performed at ±3 V sample bias and 0.1 nA tunneling current.

The calculations were performed using the density functional theory in the local density approximation (LDA), and the density matrix method of tight binding (TB). The details of the calculations can be found elsewhere (e.g., Ref. 10).

<sup>a)</sup>Electronic mail: ilan.goldfarb@materials.ox.ac.uk

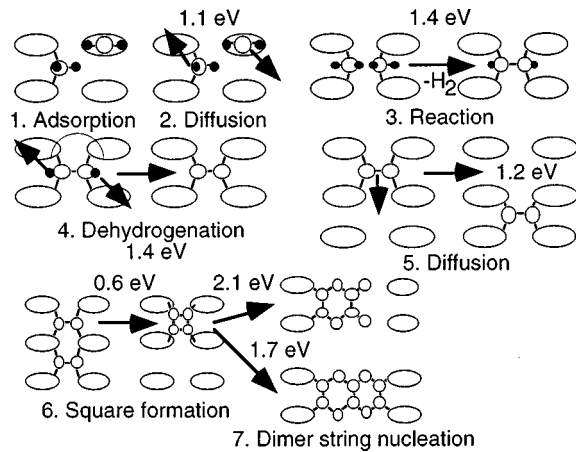


FIG. 1. Schematic diagram of the reaction pathway from disilane to silicon dimer rows. The disilane dissociates upon adsorption, as two SiH<sub>3</sub> groups, which rapidly break up into SiH<sub>2</sub> and adsorbed H. The SiH<sub>2</sub> groups can diffuse and form monohydride ad-dimers, which lose their hydrogen and rotate to form isolated epitaxial dimers. The square structures are formed from two nonrotated dimers, which may then either form the “2” structure with a high barrier, or attach an epitaxial dimer, and form a length-3 string.

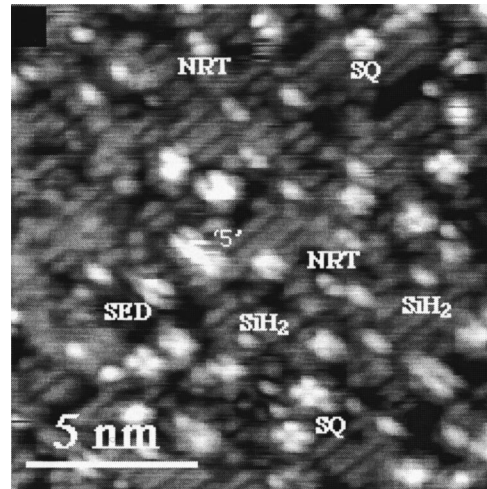


FIG. 2. Empty states STM image of the Si(001) surface after exposure to a small dose of disilane at 200 °C. In empty states, dimers have a distinctive node, which makes them easier to identify than in filled states. The square structures are marked with “SQ,” “NRT” refers to a nonrotated dimer, which has lost its hydrogen, but is oriented parallel to the substrate dimers, and “SED” refers to a silicon epitaxial dimer. Some of the SiH<sub>2</sub> groups have not reacted at this temperature. “5” refers to the length of a dimer string which has formed.

### III. RESULTS AND DISCUSSION

#### A. Nucleation of Si and Ge dimer rows

The reaction pathway to island formation from disilane (Ref. 10) is shown schematically in Fig. 1. The Si<sub>2</sub>H<sub>6</sub> molecules break up on impact into SiH<sub>3</sub> groups, which decay to form SiH<sub>2</sub>+H at room temperature.<sup>8</sup> These SiH<sub>2</sub> groups diffuse together and form nonepitaxial monohydride ad-dimers, which lose their hydrogen at 150 °C, forming nonrotated ad-dimers. Most of these ad-dimers become mobile at around 200 °C (Refs. 19 and 20) and react together to form a “square” structure,<sup>21</sup> which is the nucleus of a dimer string. A typical image of the surface after a dose of disilane at around 200 °C is shown in Fig. 2. Some SiH<sub>2</sub> groups have still not reacted, but mostly the surface features are single dimers and squares. Growth of Ge/Si(001) from germane appears to follow a very similar pathway.<sup>14</sup>

Above 250–300 °C, (Fig. 3) higher hydrides are rarely seen. Virtually all the dimers have formed into “condensed” or “diluted” (usually made of trench dimers in neighboring sites, marked with dots) rows. Dimer rows are not stable at this temperature, one may be seen “condensing” into a complete dimer row between A and B, while its neighbor has broken up. Thus, island nucleation is not an irreversible process. The vast majority of dimer strings will terminate in a trench dimer, as this maintains the rebonded configuration.<sup>10,22</sup>

This reaction pathway is quite different to that proposed for MBE.<sup>19,23–25</sup> In that case, adatoms attract one another, forming ad-atom-dimer complexes variously termed and “diluted” dimer rows<sup>24</sup> (with the dimer bonds in the nonepitaxial direction), “crosses,”<sup>25</sup> and “stealth” dimers.<sup>19</sup> These structures have never been seen in our experiments, which we believe to be due to the fact that a monohydride ad-dimer is not attractive to SiH<sub>2</sub> groups in the way that

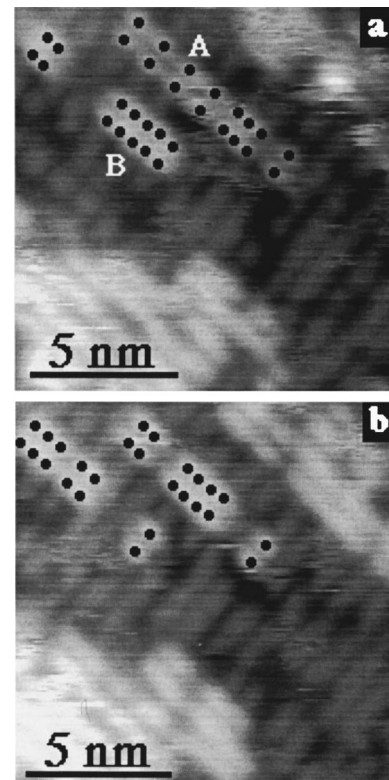


FIG. 3. Typical empty-states STM image of Si(001) surface after a short exposure, 0.2 L, to disilane at 340 °C. The positions of the dimers in two islands are marked with dots. A “diluted” dimer row, labeled A in (a), “condenses” into a complete dimer string (b) and a smaller “condensed” dimer row, labeled “B” in (a), breaks up.

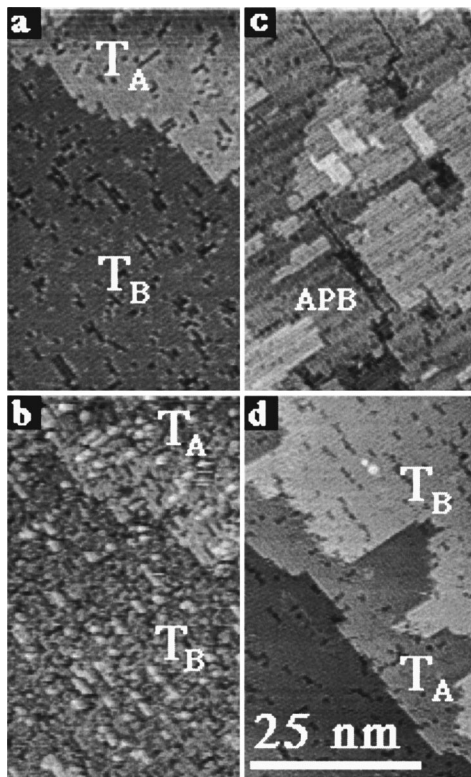


FIG. 4. Evolution of silicon surface with exposure to  $\text{Si}_2\text{H}_6$  in different growth modes. (a) Si(001) surface prior to growth, (b) surface morphology resulting from exposure to disilane at 300 °C, (c) at 340 °C, and (d) at 400 °C. The disilane pressure is  $10^{-6}$  Pa at each temperature. “ $T_A$ ” is the A-type terrace, on which the dimer rows are parallel to the down-step edge, and similarly “ $T_B$ ” is the B-type terrace, on which the dimer rows are perpendicular to the down-step edge. “APB” stands for antiphase boundary.

adatoms are. Nor have we observed trimer precursors to nucleation and  $\langle 310 \rangle$ -oriented rows, recently reported to take place in MBE experiments at RT.<sup>25</sup>

To summarize, at the low-coverage limit, no differences between silicon and germanium growth have been found. The nucleation mechanism in GSMBE is very different from that seen for MBE, however.

## B. 2D growth modes: Silicon

An intermediate growth mode of silicon from solid-source, transitional between island growth at low temperatures and true step-flow mode at high temperatures, has been very recently found by Voigtländer and co-workers.<sup>26</sup> Although these results well agree with our findings for growth from gas sources,<sup>11,14</sup> the presence of surface hydrogen imposes restriction on the minimal growth temperature. For example, at 300 °C, where Voigtländer *et al.*<sup>26</sup> observed island growth, a high density of nuclei is seen [Fig. 4(b)], but these are unable to grow because the adsorbed hydrogen blocks diffusion, and after higher exposures, the surface becomes saturated in hydrogen. Raising the temperature by only 40 °C at the same deposition pressure sufficiently activates surface diffusion and thus island growth [see Fig. 4(c)]. The first layer has been completed, and second-layer islands are

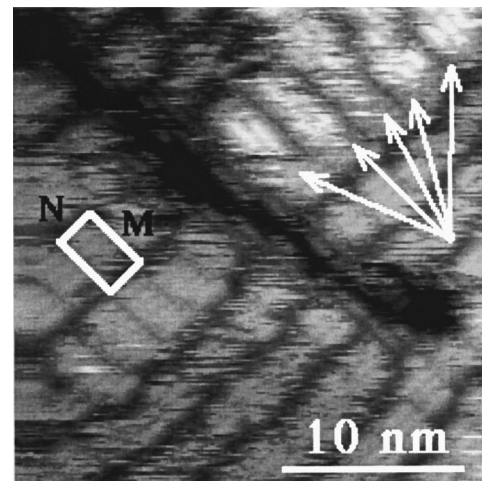


FIG. 5. Confinement of the deposited germanium to the space outlined by DVL's and DRV's, shown by the arrows. Note that while the DVL's are one dimer space wide, i.e.,  $a_0 = 4 \text{ \AA}$ , the DRV's are twice as wide, corresponding to the width of one dimer row, i.e.,  $2a_0 = 8 \text{ \AA}$ . Together they form an  $(M \times N)$  mesh, the unit cell of which is outlined.

nucleating, almost exclusively on the B-type antiphase boundaries (APBs).<sup>11,27</sup> At this temperature, no step adsorption occurs despite the obvious terrace diffusion, because the hydrogen saturates the edges of the fast-growing B-type steps, passivating them.<sup>28</sup> In general, the balance between island and step-flow growth modes is determined by the ratio between the diffusion length and terrace width, which is indeed seen in MBE.<sup>26</sup> In our experiments, the passivation of step edges with hydrogen introduces another factor into the equations. Raising the substrate temperature by a further 60 °C, above the temperature at which hydrogen desorbs from this step-edge site, leads to a transition to the step-flow growth mode, in which the size of type-B terraces increases at the expense of type-A terraces, producing a tendency for a single-domain surface as shown in Fig. 4(d). The transition to the step-flow regime is quite perfect as no islands are observed at this temperature. However, a transition back to the island mode may be observed at this temperature by increasing the gas pressure.<sup>11</sup>

## C. 2D growth modes: Germanium

We have previously shown that Ge growth from germane in the low-coverage 2D limit, in principle, follows the same three growth modes in which Si grows from disilane, i.e., H-limited growth, island growth, and step-flow growth.<sup>14</sup> In the presence of Ge, however, the tendency to stick at the edges of steps and islands is increased due to the increased hydrogen desorption from there, so that the appearance of growth is that of a mixed mode,<sup>26</sup> where island growth and step-flow growth modes coexist for the temperature at which Si grows in the purely island mode. This means that at a temperature sufficient to allow diffusion across the terraces, it is also sufficient to allow step-edge adsorption, unlike the silicon case, and therefore, there is a change in growth morphology from island growth to mixed-mode growth.

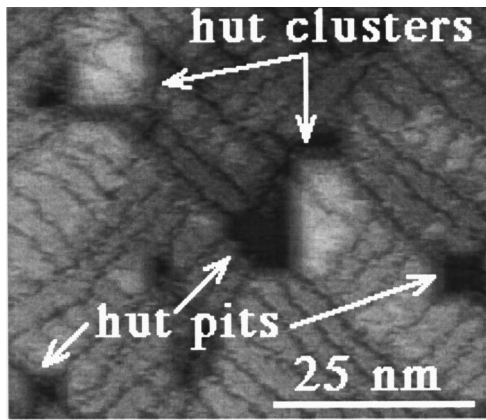


FIG. 6. The beginning of the pit $\Rightarrow$ cluster transition during growth at 420 °C. Note the split appearance of the subcritical nuclei.

Growth beyond the first monolayer and the resulting stress relaxation by the formation of dimer vacancy lines (DVL's) in a  $(2 \times N)$  structure, followed by dimer row vacancies (DRV's) in a  $(M \times N)$  structure,<sup>12,14</sup> has two interrelated implications on the growth kinetics of Ge/Si(001). In accord with theoretical predictions of an increased barrier to diffusion across DVL's,<sup>29,30</sup> films at these stages of growth demonstrate a marked reluctance to propagate the dimer rows across both defect types even at a temperature as high as 420 °C. Such a confinement on the Ge/Si(001)– $(M \times N)$  surface induces (a) island nucleation and growth between these periodic defects (see Fig. 5), on one hand, but (b) hinders the formation of APB's by greatly reducing the likelihood of islands meeting [i.e., relative to the Si(001)– $(2 \times 1)$  surface], on the other hand. Next germanium ad-dimers/adatoms have to “climb” on top of such confined islands, promoting rough growth, unlike the silicon case, where as soon as two islands meet at an APB, a new island nucleates, giving layer-by-layer growth.<sup>11,27</sup>

#### D. 3D growth

The 2D $\Rightarrow$ 3D growth transition starts when the mismatch strain can no longer be accommodated by the periodic DVL's and DRV's.<sup>12,14</sup> The presence of hydrogen has the effect of increasing the 2D layer thickness in GSMBE, at sufficiently high growth temperatures, up to 7–8 ML,<sup>14</sup> in which case strain relief by pyramidal  $\{501\}$ -faceted pits is favored (rather than by similarly faceted hut clusters), as has been theoretically predicted by Tersoff and LeGoues<sup>31</sup> and experimentally shown by Goldfarb *et al.*<sup>12</sup> However, the pit growth leads to a replacement of pits by clusters, since it requires material expulsion from the pit outwards onto the interpit layer, where this material immediately forms clusters.<sup>12</sup> Two such events of cluster nucleation from pits are shown in Fig. 6. A nonpit mediated cluster nucleation at the step edge at a lower temperature, and its growth, are shown in Fig. 7. We have previously described the special kind of heterogeneous cluster nucleation on various surface irregularities, the edges of which transform into  $\langle 100 \rangle$ -oriented segments as a precursor.<sup>12</sup> Note the short straight

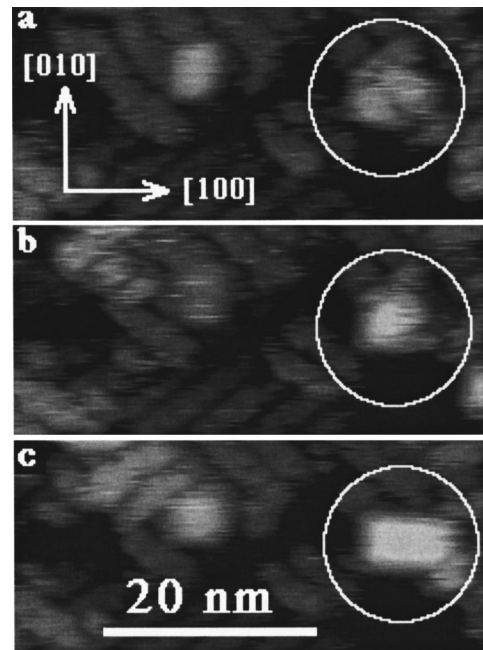


FIG. 7. Nucleation and growth of a hut cluster during Ge growth at 350 °C. Note the split appearance of the subcritical nucleus. The flat appearance of the cluster (which is actually faceted) is caused by the high contrast conditions.

step edges on which the subcritical nucleus is formed, i.e.,  $[010]$  left and  $[100]$  bottom edges, in Fig. 7(a). Here, we also want to draw attention to another interesting feature of cluster nucleation: the first 3D feature, defined by us as a “subcritical 3D nucleus,” appears to be created in a split configuration, from both sides of an existing vacancy line, as can be seen in Figs. 6 and 7(a). At the next stage these two triangular-based halves unite to produce a square-based pyramid, which we define as a “critical 3D nucleus” [see Fig. 7(b)], from which the cluster grows spontaneously, as shown in Fig. 7(c). At present, we cannot propose a complete explanation for this interesting trench-mediated nucleation; however, it is not inconceivable that the strain relief at the trench helps to compensate the initial increase in surface energy, i.e., before the elastic relaxation at the cluster apex occurs. Being able to measure the growth kinetics of individual clusters in real time, we have found the dependence of cluster size on time to obey a simple power law,<sup>13</sup>  $r \propto t^{1/5}$  (see Fig. 8). Such a low exponent, as well as the large scatter in the absolute growth constants deduced from measurements over several clusters, is inconsistent with a nucleation-controlled growth mode.<sup>13</sup> The growth proceeds by material addition to strained  $\{501\}$  cluster facets, and in the past was assumed to be controlled by the nucleation barrier on the facet, since incomplete facets were never observed.<sup>15,32</sup> However, real-time observations frequently reveal only partly completed facets,<sup>12</sup> such as those shown in Fig. 9, inconsistent with the nucleation-limited model in which once the nucleation step is completed the layer covers the facet

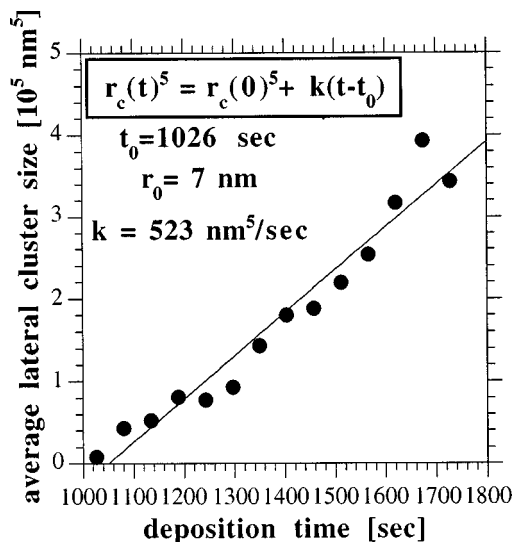


FIG. 8. Growth rate curve of the hut cluster shown in Fig. 7, in the linear representation. The full circles are the experimental measurements of the fifth power of cluster size at different times (from the growth film at 350 °C), and the full line is the linear data fit. The fitting equation and kinetic parameters, such as the critical cluster size  $r_0$  and the growth rate constant  $k$  are given in the inset. “ $t_0$ ” denotes the time to appearance of the subcritical nucleus.

very rapidly, but rather supports the model of diffusion-controlled growth in accordance with the low growth exponent.

#### IV. CONCLUSIONS

In this work, we have shown in detail nucleation and growth of Ge and Si from gas-sources on Si(001), from the formation of the first dimer strings resulting from the thermal decomposition of the gas molecules, up to several monolayers, as follows from real-time STM observations during growth. In addition to “square-” mediated nucleation of dimer strings,<sup>10,14</sup> we have also observed direct nucleation of epitaxial islands from the interaction between “diluted” dimer strings.

The particular way in which further growth of silicon proceeds is determined by the ratio of the gas flux to the substrate temperature. Up to 300 °C the surface hydrogen is immobile, leading to the “nucleation-without-growth” mode regardless of the flux used. As the diffusivity is exponentially dependent upon the substrate temperature, even a 40 °C rise is sufficient to promote island growth (almost exclusively at antiphase boundaries), and a further increase in the temperature to 400 °C allows for step-flow growth for the same pressure range. The latter mode is generally preferred, as it leads to a smoother morphology.

Although in the few-monolayer limit Ge grows two-dimensionally in a similar way, mixed-mode growth occurs preferentially over island growth due to the lower hydrogen desorption temperature, which promotes terrace diffusion, and prevents step-edge poisoning. After the first monolayer, the strain-related periodic defects hinder the formation of antiphase boundaries, and hence, reduce island nucleation on

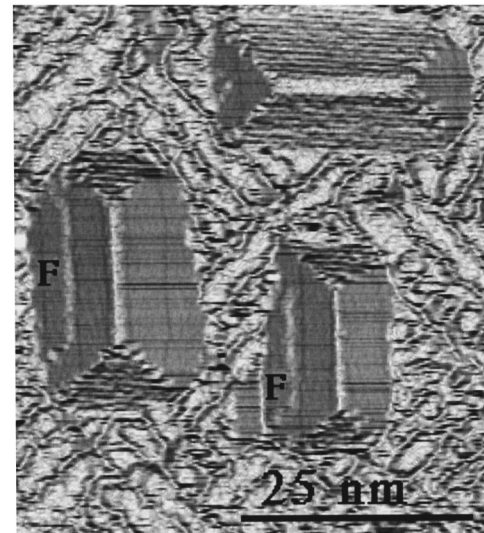


FIG. 9. Growth of hut clusters by facet nucleation (incomplete layers are marked by “F”). The image was filtered for edge enhancement.

APB’s. However, they present a barrier to diffusion to the step edges, and so favor island nucleation on terraces, whose growth is then restricted by the vacancy lines.

Unlike Si, Ge growth beyond a few monolayers results in nucleation of small and coherent three-dimensional clusters bounded by {501} facets; at higher temperatures and thicker 2D layers (due to the surfactant effect of surface hydrogen), pyramidal pits precede the clusters. The clusters nucleate heterogeneously on the  $\langle 100 \rangle$ -oriented edges of the existing surface defects by first forming subcritical nuclei split by the periodic trench defect, and then critical ones, from which the clusters grow spontaneously. The cluster growth obeys a power-law dependence on time, with the exponent around one-fifth. Such a low exponent, combined with the large scatter of growth rate constants, and observation of partially completed facets suggests diffusion-limited, rather than the commonly assumed nucleation-limited, growth.

#### ACKNOWLEDGMENTS

This work is supported by Engineering and Physical Sciences Research Council grant (EPSRC GR/K08161). Computing facilities were provided by the Materials Modelling Laboratory, Oxford. Two of the authors (J.H.G.O. and D.R.B.) were funded by the EPSRC. One of the authors (J.H.G.O.) was sponsored by AEA Technology. The authors would like to thank M. Fearn for fruitful discussions.

<sup>1</sup>D. J. Eaglesham and M. Cerullo, Phys. Rev. Lett. **64**, 1943 (1990).

<sup>2</sup>M. Hammar, F. K. LeGoues, J. Tersoff, M. C. Reuter, and R. M. Tromp, Surf. Sci. **349**, 129 (1995).

<sup>3</sup>A. J. Cullis, D. J. Robbins, A. J. Pidduck, and P. W. Smith, J. Cryst. Growth **123**, 333 (1992).

<sup>4</sup>R. Nötzel, Semicond. Sci. Technol. **11**, 1365 (1996).

<sup>5</sup>P. M. Petroff and G. Medeiros-Ribeiro, MRS Bull. **21**, 50 (1996).

<sup>6</sup>B. M. H. Ning and J. E. Crowell, Surf. Sci. **295**, 79 (1993).

<sup>7</sup>J. Spitzmüller, M. Fehrenbacher, M. Pitter, H. Rauscher, and R. J. Behm, Phys. Rev. B **55**, 4659 (1996).

<sup>8</sup>Y. Wang, M. J. Bronikowski, and R. J. Hamers, Surf. Sci. **311**, 64 (1994).

- <sup>9</sup>G. Ohta, S. Fukatsu, Y. Ebuchi, T. Hattori, N. Usami, and Y. Shiraki, *Appl. Phys. Lett.* **65**, 2975 (1994).
- <sup>10</sup>J. H. G. Owen, K. Miki, D. R. Bowler, C. M. Goringe, I. Goldfarb, and G. A. D. Briggs, *Surf. Sci.* **394**, 79 (1997).
- <sup>11</sup>J. H. G. Owen, K. Miki, D. R. Bowler, C. M. Goringe, I. Goldfarb, and G. A. D. Briggs, *Surf. Sci.* **394**, 91 (1997).
- <sup>12</sup>I. Goldfarb, P. T. Hayden, J. H. G. Owen, and G. A. D. Briggs, *Phys. Rev. Lett.* **78**, 3959 (1997).
- <sup>13</sup>I. Goldfarb, P. T. Hayden, J. H. G. Owen, and G. A. D. Briggs, *Phys. Rev. B* **56**, 10 459 (1997).
- <sup>14</sup>I. Goldfarb, J. H. G. Owen, P. T. Hayden, D. R. Bowler, K. Miki, and G. A. D. Briggs, *Surf. Sci.* **394**, 105 (1997).
- <sup>15</sup>Y.-W. Mo and M. G. Lagally, *J. Cryst. Growth* **111**, 876 (1991).
- <sup>16</sup>J. E. Vasek, Z. Y. Zhang, C. T. Salling, and M. G. Lagally, *Phys. Rev. B* **51**, 17 207 (1995).
- <sup>17</sup>E. Kaxiras, *Surf. Rev. Lett.* **3**, 1295 (1996).
- <sup>18</sup>D. Kandel, *Phys. Rev. Lett.* **78**, 499 (1997).
- <sup>19</sup>B. Borovsky, M. Krueger, and E. Ganz, *Phys. Rev. Lett.* **78**, 4229 (1997).
- <sup>20</sup>C. M. Goringe and D. R. Bowler, *Phys. Rev. B* **56**, R7073 (1997).
- <sup>21</sup>J. H. G. Owen, D. R. Bowler, C. M. Goringe, K. Miki, and G. A. D. Briggs, *Surf. Sci. Lett.* **382**, L678 (1997).
- <sup>22</sup>C. Pearson, M. Krueger, and E. Ganz, *Phys. Rev. Lett.* **76**, 2306 (1996).
- <sup>23</sup>Y.-W. Mo, R. Kariotis, B. S. Swartzentruber, and M. G. Lagally, *J. Vac. Sci. Technol. A* **8**, 201 (1990).
- <sup>24</sup>P. J. Bedrossian, *Phys. Rev. Lett.* **74**, 3648 (1994).
- <sup>25</sup>J. van Wingerden, A. van Dam, M. J. Haye, P. M. L. O. Scholte, and F. Tuinstra, *Phys. Rev. B* **55**, 4723 (1997).
- <sup>26</sup>B. Voigtländer, T. Weber, P. Smilauer, and D. E. Wolf, *Phys. Rev. Lett.* **78**, 2164 (1997).
- <sup>27</sup>M. J. Bronikowski, Y. Wang, and R. J. Hames, *Phys. Rev. B* **48**, 12 361 (1993).
- <sup>28</sup>D. R. Bowler, J. H. G. Owen, C. M. Goringe, K. Miki, and G. A. D. Briggs (unpublished).
- <sup>29</sup>C. Roland and G. H. Gilmer, *Phys. Rev. B* **47**, 16 286 (1992).
- <sup>30</sup>B. D. Yu and A. Oshiyama, *Phys. Rev. B* **52**, 8337 (1995).
- <sup>31</sup>J. Tersoff and F. K. LeGoues, *Phys. Rev. Lett.* **72**, 3570 (1994).
- <sup>32</sup>Y.-W. Mo, D. E. Savage, B. S. Swartzentruber, and M. G. Lagally, *Phys. Rev. Lett.* **65**, 1020 (1990).